arXiv:cond-mat/0505356v1 [cond-mat.mtrl-sci] 13 May 2005

Magnetization Reversal in Elongated Fe Nanoparticles

Yongqing Li,* Peng Xiong, and Stephan von Molnár
MARTECH and Department of Physics, Florida State University, Tallahassee, FL 32306-4351

Yuzo Ohno and Hideo Ohno
Laboratory for Nanoelectronics and Spintronics, Research Institute of Electrical Communication, Tohoku University, Sendai, Japan

(Dated: March 23, 2022)

Magnetization reversal of individual, isolated high-aspect-ratio Fe nanoparticles with diameters comparable to the magnetic exchange length is studied by high-sensitivity submicron Hall magnetometry. For a Fe nanoparticle with diameter of 5 nm, the magnetization reversal is found to be an incoherent process with localized nucleation assisted by thermal activation, even though the particle has a single-domain static state. For a larger elongated Fe nanoparticle with a diameter greater than 10 nm, the inhomogeneous magnetic structure of the particle plays important role in the reversal process.

PACS numbers: 75.75.+a, 85.75.Nn, 75.60.Jk, 75.60.Ch

I. INTRODUCTION

Magnetic nanowires still attracted much attention despite a long history of the study of elongated magnetic nanoparticles[1]. Besides some potential technological applications such as high density magnetic information storage, magnetic nanowires also provide a unique arena for testing theoretical models of magnetization reversal. Recent work on magnetization reversal[2,3] and domain wall motion[4,5] in magnetic nanowires has provided in-depth understanding of magnetism on the nanometer scale and even atomic scales. In a magnetic nanowire, the competition between the magnetostatic energy and magnetic exchange interaction gives rise to a characteristic length, the coherence diameter, $d_c \simeq 7.3 l_{ex} = 7.3(A/4\pi M_s)^{1/2}$, where l_{ex} is the magnetic exchange length, A the exchange constant and M_s the saturation magnetization[6]. For Fe, Co, and Ni, d_c is about 11, 15 and 25 nm, respectively[1]. For an ideal nanowire with diameter $d \ll d_c$, micromagnetic theory predicts a coherent rotation of the entire magnetic volume due to the dominance of exchange interactions, while incoherent reversal modes such as curling are favored for nanowires with $d > d_c$[7]. A large body of experimental results on magnetic nanowires have been analyzed in terms of these fundamental reversal modes. Most of the measurements, however, were carried out on ensembles of magnetic nanowires, in which data analysis is complicated by the distribution of size, shape, and microstructure of the nanowires, as well as the dipolar interaction between the nanowires. In addition, some important properties of individual particles such as the stochastic nature of magnetization reversal are averaged out. Measurements on single magnetic nanowires have only been reported in a few cases. For example, electrodeposited Ni or Co nanowires with diameters between 30 nm and 90 nm were studied with micro-SQUID magnetometers[2] and subsequently by utilizing the anisotropic magnetoresistance (AMR) effect[3,8]. Experimental data from these measurements have been fitted to the curling mode, but difficulty arises due to the fact that the anisotropy energy from magnetocrystalline and/or other effects are comparable to the shape anisotropy[3,8]. Hence, the study of individual nanowires with one dominant anisotropy could provide further insight into the fundamental magnetization reversal process in such magnetic nanostructures. The Fe nanowires are one of the ideal systems because their shape anisotropy is at least one order of magnitude larger than the magnetocrystalline and strain anisotropies[9,10].

In this paper, we report the first detailed study of *individual* cylinder-shaped Fe nanoparticles with diameters close to the coherence diameter. Measurements of a single Fe nanocylinder with $d \simeq 5$ nm reveals the incoherent and localized nature of the magnetization reversal although the particle has a single-domain static state. We also present the results on an elongated Fe nanoparticle with more structural imperfections, as the first step toward studying more complex magnetic dynamics in nanowires with diameters on the 10 nm scale.

II. EXPERIMENT

Cylinder-shaped Fe nanoparticles were fabricated with a scanning tunneling microscopy (STM) assisted chemical vapor deposition technique, in which a precursor, $Fe(CO)_5$, was decomposed by applying a high bias voltage to the STM tip[11,12]. Growth was controlled by the STM feedback electronics operated in constant tunneling current mode. The fabricated Fe nanoparticles have a polycrystalline bcc iron core surrounded by an amorphous carbon coating[12], which effectively prevents the sample from oxidation[13]. The diameter of the iron core can be varied from a few nm to 20 nm by varying the growth rate, which can be controlled by the precursor pressure[12,14]. The height of the Fe particles can be precisely controlled by withdrawing the piezoelectric scan-

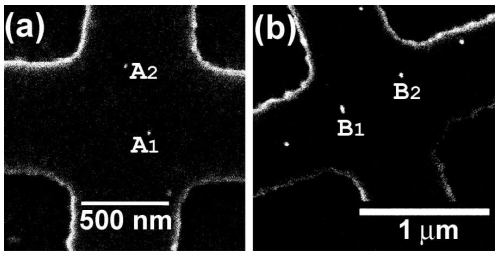


FIG. 1: SEM images of two samples suitable for measurements of single cylinder-shaped Fe nanoparticles with $h \simeq 120\,\mathrm{nm}$. The stray field from the Fe particles is sensed by $0.6{\times}0.6\,\mu\mathrm{m}^2$ GaAs/AlGaAs Hall magnetometers. (a) The growth time for particles A_1 and A_2 is 11 s. The diameter of particle A_1 is estimated to be 5 nm. (b) The growth time for particles B_1 and B_2 are 42 s and 35 s, respectively.

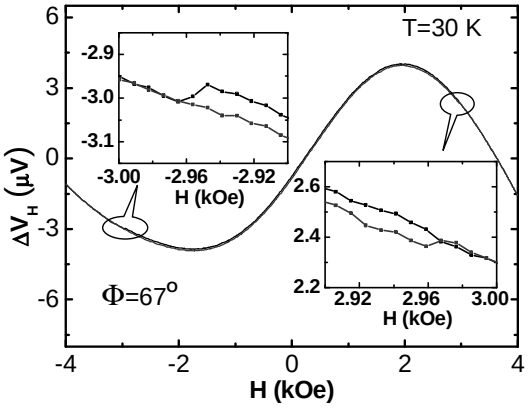


FIG. 2: A typical hysteresis curve of sample (a) from the Hall gradiometry measurement at $T = 30\,\mathrm{K}$ with magnetic filed applied 67 ° relative to the easy axis. The two insets are the close-up view of magnetization reversals of the particle A_1.

ning tube after it reaches a predetermined setpoint and can be varied from tens of nanometers to a few microns[12]. In order to measure a single Fe nanoparticle, we grew a small number of Fe nanoparticles with very large spacing onto a submicron Hall magnetometer fabricated from a GaAs/AlGasAs heterostructure. The heterostructure is consisted of a $1\,\mu$m undoped GaAs layer, a 30 nm $Al_{0.33}Ga_{0.67}As$ spacer, a 80 nm n-doped $Al_{0.33}Ga_{0.67}As$ layer, and a 5 nm GaAs cap. The carrier concentration and the mobility of the two-dimensional electron gas (2DEG) in this heterostructure are $n = 2.2 \times 10^{11}\,\mathrm{cm}^2$ and $\mu = 1 \times 10^5\,\mathrm{cm}^2/\mathrm{V{\cdot}s}$, respectively, which were measured in the dark at $T = 77\,\mathrm{K}$. The STM-assisted growth technique offers the critical high precision positioning capability which makes the measurement of single nanoparticles possible.

Shown in Fig. 1 are scanning electron microscopy (SEM) images of two samples to be presented in this paper. The height of the particles was set to be $h \simeq 120\,\mathrm{nm}$, so the easy axis of the particles is nearly perpendicular to the 2DEG plane due to the dominance of shape anisotropy ($h \gg d$). The particles in sample (a) were grown at a faster rate than those in sample (b), so the diameters of particles A_1 and A_2 are expected to be smaller than those of particles B_1 and B_2[12]. The size of the Hall crosses in both samples, which were fabricated with electron beam lithography followed by wet chemical etching, is about $0.6 \times 0.6\,\mu\mathrm{m}^2$. By proper gating of the 2DEG, and using a gradiometry setup in which the differential Hall voltage between an empty Hall cross and a Hall cross with nanoparticles grown on top is measured[15,16], moment sensitivity of submicron magnetometers has been improved to better than $10^4\,\mu_B/\mathrm{Hz}^{1/2}$ at 1 Hz in a large applied magnetic field[17]. The advantages of Hall magnetometry over other single particle measurement techniques include the wide range of operational temperature, no limitation in applied fields, as well as the non-invasive nature of the measurement.

III. RESULTS AND DISCUSSION

Hundreds of Hall measurements have been performed on sample (a) at various temperatures and applied field angles (Earlier results on this sample with field applied parallel to the easy axis of the Fe nanoparticle were presented in Ref. [18]). In each of the measurements, only one sharp jump in the Hall signal corresponding to the switching of one particle is detected. Fig. 2 shows a typical hysteresis curve (raw data) measured at $T = 30\,\mathrm{K}$ and $\Phi = 67\,°$, where Φ is the angle between the applied magnetic field and the easy axis of the Fe nanoparticle. The large nonlinear background originates from the mesoscopic effects in the small 2DEG structure at low temperatures. The observation of the switching of one particle instead of two is not surprising: from simple calculations the Hall signal from particle A_1 is estimated to be about one order of magnitude larger than that of particle A_2. In fact, the signal from particle A_2 is below the noise level and thus undetectable in our measurements. When the magnetic field is applied parallel to the easy axis, the net hysteresis curve, obtained by subtracting the nonlinear background, has a nearly rectangular shape[18]. From the Hall signal at zero field, the magnetic moment of the particle is extracted from its average stray field over the active area of Hall cross ($\sim 0.4 \times 0.4\,\mu\mathrm{m}^2$). The diameter of particle A_1 is estimated to be 5 ± 1 nm, which is much smaller than the coherence diameter of Fe nanowires (11 nm). The dominance of exchange interaction at this length scale favors a single domain structure. Indeed, we found that the hysteresis curve of this particle is independent of field sweep history as long as the field is swept from above the switching fields, suggesting that this cylinder-shaped particle is a single-domain particle at least by the static definition[19].

The magnetization reversal of a perfect nanowire with $d < d_c$ can be described by coherent rotation. The cor-

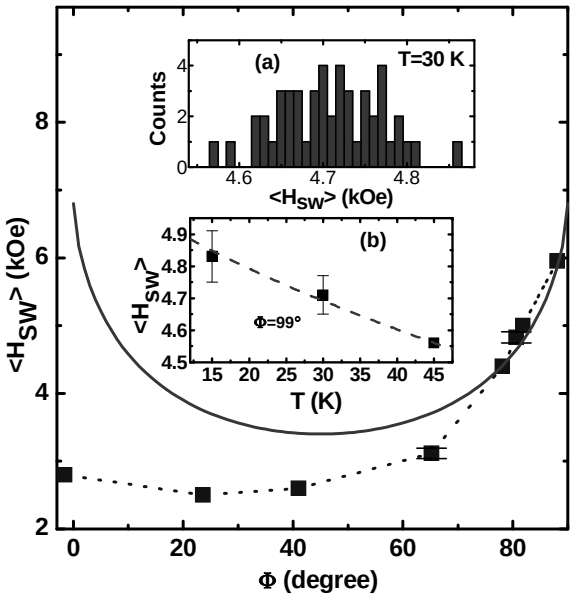


FIG. 3: The angular dependence of the average switching fields, $\langle H_{sw}\rangle$, of particle A_1 at $T = 30\,\mathrm{K}$. Inset (a) shows the wide distribution of the switching fields at $\Phi = 99\,^\circ$ and $T = 30\,\mathrm{K}$. Inset (b) is the temperature dependence of $\langle H_{sw}\rangle$ at $\Phi = 99\,^\circ$. The spreading width of the switching fields is shown by the height of the bars in inset (b), which is the statistical standard deviation of H_{sw} obtained from the histogram measurements.

responding angular dependence of the switching fields is well described by the Stoner-Wohlfarth model[20], and can be written as $H_{sw} = H_K(\sin^{2/3}\Phi + \cos^{2/3}\Phi)^{-3/2}$, where H_K is the anisotropy field. As shown in Fig. 3, the measured angular dependence of the switching fields of particle A_1 deviates significantly from that expected from coherent rotation. The switching fields at lower angles are much lower than those for coherent rotation. At high angles, the switching fields decrease rapidly with decreasing Φ, which is similar to previous results on Fe nanoparticle arrays with d = 7-14 nm[13,21]. Nonetheless, we notice that the switching field at $\Phi \sim 25\,^\circ$ appears to be slightly lower than that at $\Phi \simeq 0\,^\circ$, which might be regarded as a weak signature of coherent rotation suggested in Ref. [2] for similar effects in Ni nanowires. Such a feature was not observed in our previous measurements on Fe nanoparticle arrays[13,21].

The deviation from coherent rotation is further manifested in the histogram measurements. The stochastic nature of the switching process causes the spreading of the switching fields in a certain range. In the Néel-Brown model[22,23], the magnetization reversal of a dynamic single domain particle at finite temperature is described as thermal activation over a single energy barrier. Kurkijärvi developed a formalism mathematically connecting the switching statistics to the energy barrier[24]. Measurements on individual ellipsoidal Co nanoparticles of d = 25 nm by Wernsdorfer et al. provided the first experimental agreement with the Néel-Brown model[25]. This model predicts an increase of the spreading width and a decrease in the average switching field $\langle H_{sw}\rangle$ with increasing temperature. This is not the case for particle A_1. As shown in the inset of Fig. 3, the spreading width does not increase with temperature. The spreading width estimated from Kurkijärvi's formulas is at least one order of magnitude smaller than our experimental value (∼2% of the H_{sw} at T=15 K). Similar wide distribution of H_{sw} has also been observed in electrodeposited Ni nanowires with d=75 nm[2]. The observed $\langle H_{sw}\rangle$ does decrease with temperature as expected from thermal activation, but it decreases much faster than the prediction of the Néel-Brown model. The extracted energy barrier, E_0, is 3×10^4 K from the data at $\Phi = 99\,^\circ$ and T = 15-45 K (inset b in Fig. 3), corresponding to a thermal activation volume of $\sim 5 \times 10^2\,\mathrm{nm}^3$, which is only about 1/5 of the total volume of the nanocylinder. This is consistent with previous magnetic viscosity measurements on large arrays of similar Fe nanoparticles, in which the thermal activation volume was also found to be a small fraction of the particles' total volume[14]. Similar results were also reported on electrodeposited Ni nanowires[2].

The data presented above clearly suggest that the magnetization reversal of particle A_1 is an incoherent process in which the nucleation is localized and thermally assisted, despite the fact that this particle has a diameter smaller than the coherence diameter. Recent micromagnetic simulation of defect-free d=9 nm Fe nanopillars by Brown et al.[26,27] showed that nucleation can start at both ends and propagate through the whole pillars in the time scale of nanoseconds. The calculated H_{sw} is about 2 kOe for the fields applied parallel to the easy axis, which is close to our experimental value. Another theoretical work by Skomski et al. found that disorder such as structural imperfections favor the localized magnetization reversal over the delocalized modes such as coherent rotation and curling[28]. The Fe nanoparticles fabricated with STM are polycrystalline[12], so multiple nucleation sites including both the ends and the imperfections (e.g. grain boundaries) are probably involved in the switching process. On the other hand, the single-domain static state of this particle suggests that these defects are still not strong enough to serve as pinning centers for domain walls, which are overwhelmed by magnetic exchange between strongly interacting magnetic clusters (grains) favoring a uniform spin distribution. It will be of particular interest to study how these structural imperfections affect the propagation process after the nucleation, which may determine the ultimate speed of spintronic devices based on such elongated nanoparticles or similar nanostructures.

Recently spintronic devices based on manipulation of domain walls have been proposed[29]. A reduction of domain wall velocity with decreasing feature size has been reported recently in submicron stripes of ultrathin Pt/Co/Pt films[5]. As a first step toward the study of domain wall motion on the 10 nm scale, we now demonstrate that elongated Fe nanoparticles with do-

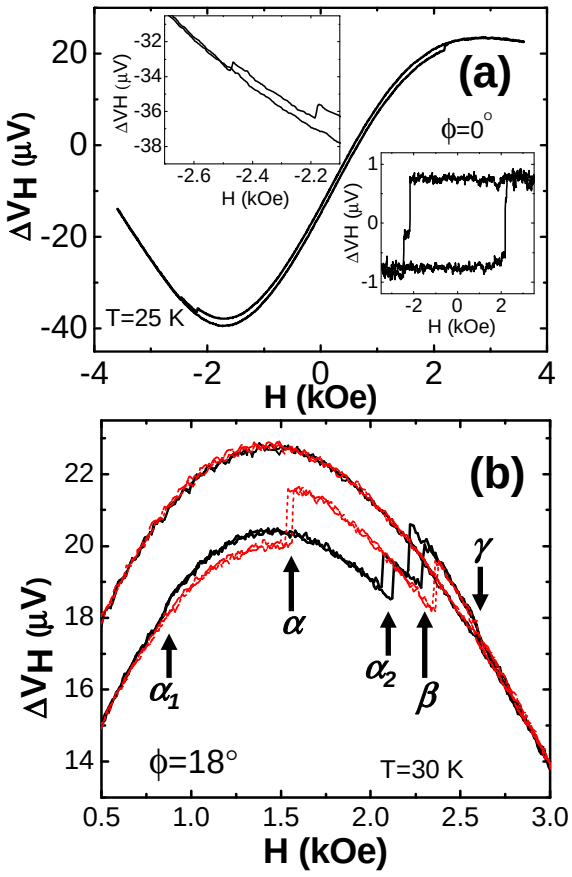


FIG. 4: (Color online) (a) The hysteresis curve of the sample (b) at $T = 25\,\mathrm{K}$ and with magnetic field applied perpendicular to the substrate. The upper-left inset is the close-up view of the magnetic switching. The lower-right inset shows the net hysteresis curve after the subtraction of non-linear background. (b) Part of four hysteresis loops of the same sample taken at $T = 30\,\mathrm{K}$ and with fields applied 18 ° relative to the normal of the substrate, i.e. $\phi = 18\,^\circ$. Two loops (black lines) have four switching events (α_1, α_2, β, and γ), while the other two (red (dark gray) lines) have three (α, β, and γ).

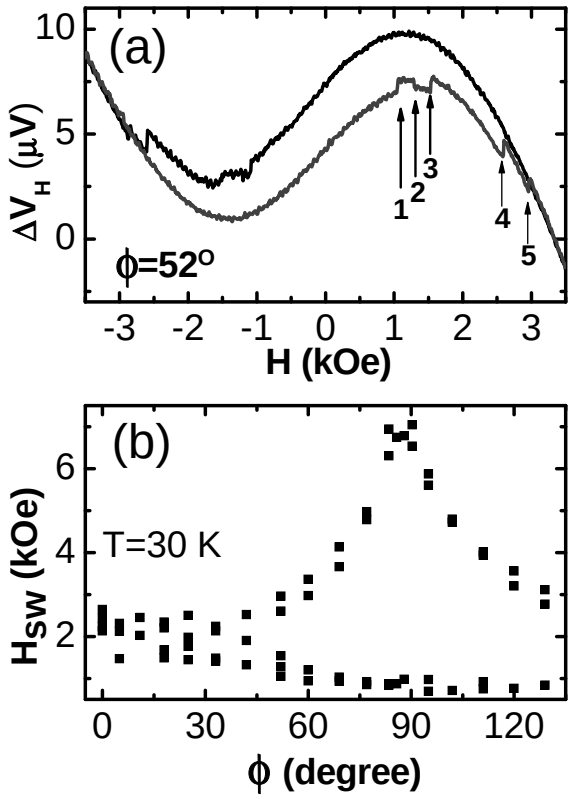


FIG. 5: A typical hysteresis curve of particle B_1 obtained at $\phi = 52\,^\circ$ and $T = 30\,\mathrm{K}$, which shows five switching events as the field is swept up. (b) Angular dependence of the switching fields of the same particle at $T = 30\,\mathrm{K}$.

main walls can be fabricated with the STM-CVD technique. Fig. 4(a) shows the hysteresis curve of the sample (b) taken at $T = 25\,\mathrm{K}$ and with the field applied nearly parallel to the easy axis, in which only two particles (B_1 and B_2) are close to the active region of the Hall cross. After subtraction of the nonlinear background, we obtain a rectangular shaped net hysteresis curve, shown in the lower-right inset of Fig. 4(a), which exhibits two distinct sharp jumps in the Hall signal. We attribute these two jumps to the magnetization reversal of the particle B_1 alone, instead of both particles B_1 and B_2, based on the following experimental results: (1) although the sum of the two jumps in the Hall signal corresponding to the two magnetization reversals, $\Delta V_{H1} + \Delta V_{H2}$, remains constant, the ratio, $\Delta V_{H1}/\Delta V_{H2}$, varies from 1.1 to 1.9 in different measurements; (2) The size of particle B_2 is expected to be smaller than particle B_1, and the location of particle B_2 is more off-center than particle B_1, so the contribution of particle B_2 to the Hall signal, if observable, would be smaller than that of particle B_1. From the Hall signal, we estimate that the diameter of particle B_1 to be about 10-15 nm[30].

The inhomogeneous nature of the particle is further evidenced by the measurements in tilted fields. Fig. 4(b) shows part of four hysteresis loops taken at exactly the same conditions ($\phi = 18\,^\circ$ and $T = 30\,\mathrm{K}$). Among them, two loops have four switching events (α_1, α_2, β, and γ), while the other two only have three (α, β, and γ). Similar stochastic switching behavior has also been observed at other field tilting angles. The number of switching events for each magnetization reversal varies from two to as many as five [Fig. 5(a)]. The angular dependence of the switching fields for a typical field sweep is plotted in Fig. 5(b). The distribution of switching fields shows a very complex behavior. Nonetheless, the switching fields at high angles ($\phi > 50\,^\circ$) are divided into two distinctive groups: a soft group (with lower switching fields) having a weak angular dependence and a hard group with a strong angular dependence similar to that for a typical single-domain elongated Fe nanoparticle such as particle A_1. The multiple switching events and their angular dependence suggest that the soft portion of particle B_1 is probably composed of interacting clusters with varying

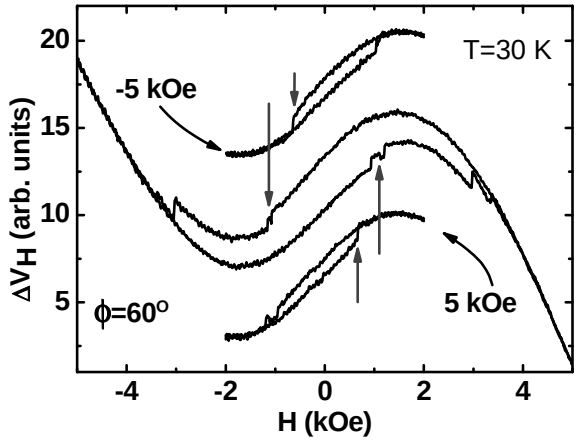


FIG. 6: Three hysteresis loops of particle B_1 with different field sweep histories. The middle curve has a history $-5\,\mathrm{kOe}\rightarrow 5\,\mathrm{kOe}\rightarrow -5\,\mathrm{kOe}$, in which both the soft and the hard portions of the particle are switched. The upper and lower curves correspond to $(-5\,\mathrm{kOe})\rightarrow -2\,\mathrm{kOe}\rightarrow 2\,\mathrm{kOe}\rightarrow -2\,\mathrm{kOe}$, and $(5\,\mathrm{kOe})\rightarrow 2\,\mathrm{kOe}\rightarrow -2\,\mathrm{kOe}\rightarrow 2\,\mathrm{kOe}$, respectively, in which only the magnetization reversal of the soft portion occurs.

easy axes. The magnetic structure of this particle can be modified by changes in the field sweep history, which is illustrated in Fig. 6: As the field is swept between $-5\,\mathrm{kOe}$ and $5\,\mathrm{kOe}$, switching of both the soft and the hard portions takes place (middle curve). On the other hand, the upper and the lower hysteresis curves correspond to field sweeps between $-2\,\mathrm{kOe}$ and $2\,\mathrm{kOe}$, in which only the magnetization of the soft portion switches. These two curves were taken under the same conditions except for the starting field: the upper and lower curves were obtained after the field was ramped to $-5\,\mathrm{kOe}$ and $5\,\mathrm{kOe}$, respectively. The overall features of the two hysteresis curves are very similar, however, neither is symmetric with respect to $H = 0$. They are shifted in opposite directions in H, resulting in a large difference ($\sim 0.3\,\mathrm{kOe}$) in the switching fields. The observed large difference in H_{sw} of the soft portion can clearly be attributed to the difference in the magnetization direction of the particle's hard portion. Accordingly, the configuration of the domain wall(s) between the soft portion and hard portion is varied due to different field sweep history, which in turn has a large effect on the switching of neighboring domains through the exchange interaction. It should be noted that multiple switching jumps have also been observed in electrodeposited Ni[2] and permalloy[10] nanowires with $d = 30$-$90\,\mathrm{nm}$ to which the curling mode would be applicable if the nanowires were perfect.

The existence of domain walls in particle B_1 and its absence in particle A_1 as well as Fe nanowires of larger size prepared by electrodeposition[31] can be attributed to the growth process. The growth of particle B_1 was performed with lower precursor pressure and its growth rate was only about 1/4 of that of particle A_1. The growth of the Fe nanoparticles is sustained by maintaining a constant tunneling current (typically $50\,\mathrm{pA}$), so a slower growth rate is likely to produce more structural defects since the growth process suffers more external (mechanical and electronic) interference. Some of these imperfections provide the pinning forces for the domain walls. Depending on temperature, applied fields, and the strength of each pinning center, a domain wall may or may not be pinned down at a particular place, resulting in stochastic behavior of the magnetization reversal. Furthermore, the larger diameter of particle B_1 may also be responsible for the observed multi-domain structure due to the less dominant exchange interaction. Finally, we speculate that there is a slight possibility that there exists some degree of surface oxidation which would provide extra pinning forces and nucleation sites for particle B_1[32]. These surface interactions might also provide a possible explanation for the observed asymmetry in the hysteresis loops at low temperatures. A quantitative analysis of these effects, however, requires detailed information on the microstructure of the nanoparticles, which is not possible with our current experimental setup.

IV. CONCLUSION

In summary, two types of elongated Fe nanoparticles with diameter close to the coherence diameter have been studied in detail. One has a single domain static state, but the magnetization reversal cannot be described with coherent rotation. The data suggest a thermally activated nucleation and propagation process, in which possible nucleation sites include the ends and imperfections of the nanocylinder. The other type of Fe particles studied in this work has a multi-domain structure and shows complicated magnetization reversal behavior. We have demonstrated that the domain structure in these Fe nanoparticles can be manipulated through the magnetic field history. The capability of submicron Hall magnetometry in detecting the magnetization reversal of single domains on the sub-10 nm scale demonstrated in this work is promising for important applications in understanding the fundamental physics at dimensions comparable to magnetic exchange lengths, as well as nascent fields such as bio-sensing and non-invasive detection of spin-polarized carriers injected into semiconductors.

V. ACKNOWLEDGEMENTS

Y. L. gratefully thanks R. Kallaher, S. Wirth and A. Anane for technical help. This work was supported by NSF grant #DMR0072395, by DARPA through ONR grants #N-00014-99-1-1094 and #MDA-972-02-1-0002, and by FSU Research Foundation through a PEG grant. The work at Tohoku University was supported partially by a Grant-in-Aid from the Ministry of Education, Japan, and by the Japan Society for the Promotion of Science.

* Electronic address: yqli@physics.ucsb.edu

[1] D. J. Sellmyer, M. Zheng, and R.Skomski, J. Phys. Condens. Matter **13**, R433 (2001).

[2] W. Wernsdorfer, B. Doudin, D. Mailly, K. Hasselbach, A. Benoit, J. Meier, J. P. Ansermet, and B. Barbara, Phys. Rev. Lett. **77**, 1873 (1996).

[3] J.-E. Wegrowe, D. Kelly, A. Franck, S. E. Gilbert, J. P. Ansermet, Phys. Rev. Lett. **82**, 3681 (1999).

[4] O. Pietzsch, A. Kubetzka, M. Bode, R. Wiesendanger, Science **292**, 2053 (2001).

[5] F. Cayssol, D. Ravelosona, C. Chappert, J. Ferré, and J. P. Jamet, Phys. Rev. Lett. **92**, 107202 (2004).

[6] The definition of the magnetic exchange length is varied by a numerical factor in some literature.

[7] A. Aharoni, *Introduction to the Theory of Ferromagnetism*, (Oxford Press, Oxford, UK, 1996).

[8] S. Pignard, G. Goglio, A. Radulescu, L. Piraux,S. Dubois, A. Declémy, and J. L. Duvail, J. Appl. Phys. **87**, 824 (2000).

[9] A. H. Morrish, *The Physical Properties of Magnetism*, (Wiley, New York, 1965).

[10] Permalloy nanowires could be another system with dominating shape anisotropy energy. See, e.g. A. Sokolov, R. Sabirianov, W. Wernsdorfer, and B. Doudin, J. Appl. Phys. **91**, 7059 (2002).

[11] M. A. McCord, and D. D. Awschalom, Appl. Phys. Lett. **57**, 2153 (1990).

[12] A. D. Kent, T. M. Shaw, S. von Molnár, and D. D. Awschalom, Science **262**, 1249 (1993).

[13] S. Wirth, S. von Molnár, M. Field, and D. D. Awschalom, J. Appl. Phys. **85**, 5249 (1999).

[14] S. Wirth,A. Anane, and S. von Molnár, Phys. Rev. B **63**, 012402 (2001).

[15] A. D. Kent, S. von Molnár, S. Gider, and D. D. Awschalom, J. Appl. Phys. **76**, 6654 (1994).

[16] Y. Li, C. Ren, P. Xiong, S. von Molnár, Y. Ohno, and H. Ohno, Phys. Rev. Lett. **93**, 246602 (2004).

[17] Y. Q. Li, Ph. D. Thesis, Florida State University, 2003.

[18] Y. Q. Li, P. Xiong, S. von Molnár, S. Wirth, Y. Ohno, and H. Ohno, Appl. Phys. Lett. **80**, 4644 (2002).

[19] F. G. Monzon,D. S. Patterson, and M. L. Roukes, J. Magn. Magn. Mater. **195**, 19 (1999).

[20] E. C. Stoner, and E. P. Wohlfarth, Philos. Trans. Roy. Soc. London A **240**, 599 (1948).

[21] Y. Q. Li, P. Xiong, S. von Molnár, Y. Ohno, and H. Ohno, J. Appl. Phys. **93**, 7912 (2003).

[22] L. Néel, Ann. Geophys. **5**, 99 (1949).

[23] W. F. Brown, Phys. Rev. **130**, 1677 (1963).

[24] J. Kurkijärvi, Phys. Rev. B **6**, 832 (1972).

[25] W. Wernsdorfer, E. B. Orozco, K. Hasselbach, A. Benoit, B. Barbara, N. Demoncy, A. Loiseau, H. Pascard, and D. Mailly, Phys. Rev. Lett. **78**, 1791 (1997).

[26] G. Brown,M. A. Novotny, and P. A. Rikvold, Phys. Rev. B **64**, 134422 (2001).

[27] G. Brown, S. M. Stinnett, M. A. Novotny, and P. A. Rikvold, J. Appl. Phys. **95**, 6666 (2004).

[28] R. Skomski, H. Zeng, M. Zheng and D. J. Sellmyer, Phys. Rev. B **62**, 3900 (2000).

[29] D. A. Allwood, G. Xiong, M. D. Cooke, C. C. Faulkner, D. Atkinson, N. Vernier, and R. P. Cowburn, Science **296**, 2003 (2002).

[30] A more accurate estimate of the diameter of particle B_1 is very difficult because this particle is located very close to the corner of the Hall cross.

[31] T. G. Sorop, C. Untiedt, F. Luis, M. Kröll, M. Rasa, and L. J. de Jongh, Phys. Rev. B **67**, 014402 (2003).

[32] R. H. Kodama, A. E. Berkowitz, E. J. McNiff, Jr., and S. Foner, Phy. Rev. Lett. **77**, 394 (1996).